MATING SYSTEMS

A single gene orchestrates androgen variation underlying male mating morphs in ruffs

Jasmine L. Loveland[1,2]*†, Alex Zemella[1,3]*†, Vladimir M. Jovanović[3,4], Gabriele Möller[5], Christoph P. Sager[6], Bárbara Bastos[3,7], Kenneth A. Dyar[5], Leonida Fusani[2,8], Manfred Gahr[1], Lina M. Giraldo-Deck[1], Wolfgang Goymann[1,9], David B. Lank[10], Janina Tokarz[5], Katja Nowick[3], Clemens Küpper[1]*

Androgens are pleiotropic and play pivotal roles in the formation and variation of sexual phenotypes. We show that differences in circulating androgens between the three male mating morphs in ruff sandpipers are linked to 17-beta hydroxysteroid dehydrogenase 2 (HSD17B2), encoded by a gene within the supergene that determines the morphs. Low-testosterone males had higher *HSD17B2* expression in blood than high-testosterone males, as well as in brain areas related to social behaviors and testosterone production. Derived HSD17B2 isozymes, which are absent in high-testosterone males but preferentially expressed in low-testosterone males, converted testosterone to androstenedione faster than the ancestral isozyme. Thus, a combination of evolutionary changes in regulation, sequence, and structure of a single gene introduces endocrine variation underlying reproductive phenotypes.

Testosterone is instrumental for the development of the male reproductive tract, sperm production, secondary sex characteristics, skeletal muscle mass, and expression of social behaviors, including those that are sexual, aggressive, and courtship-related (*1*–*5*). Although both sexes produce testosterone, males generally have higher circulating testosterone concentrations than females (*4*, *6*–*8*). In males, testosterone is synthesized primarily in the testes, with its production controlled through a feedback-control loop in the hypothalamic-pituitary-gonadal (HPG) axis. Male testosterone levels typically peak during the breeding season (*9*, *10*) but vary considerably between individuals depending on life history, reproductive trade-offs, and alternative mating tactics (*2*, *11*, *12*). Usually, dominant territorial males have high levels of circulating testosterone while subdominant males or males that use alternative mating tactics, such as sneaking, have low testosterone levels (*11*).

Testosterone levels fluctuate diurnally and seasonally, but a proportion of the variation between individuals may have a genetic basis and quantitative genetic studies have suggested substantial heritability for testosterone in tetrapods (*13*). In humans, 65% of variation in serum testosterone concentrations between male twins was explained by genetics (*14*). Genome-wide association studies provided a number of candidate genes for testosterone variation including the sex-hormone binding globulin locus and multiple loci on the X chromosome (*8*, *15*, *16*). In addition, genes expressed along the HPG and hypothalamic-pituitary-adrenal (HPA) axes have been studied for their contributing roles to the rate of testosterone production and metabolism (*17*, *18*), including the use of prohormones such as dehydroepiandrosterone to avoid costs of high circulating testosterone (*19*). However, a detailed characterization of genetic variants linked to testosterone concentrations, including a confirmation of functional effects on testosterone production or metabolism, has so far remained elusive.

Species with multiple reproductive morphs often exhibit systemic androgen variation between male types. Ruffs (*Calidris pugnax*) feature three mating morphs that are fixed for life: independents, satellites, and faeders. The morphs show nearly discrete differences in size, plumage ornamentation, aggressive behavior, and courtship behavior (*20*) (Fig. 1, A and B). During the mating season, males of the most common independent morph compete aggressively with each other to establish a dominance hierarchy on leks. The most competitive independents display on small lek courts to entice visiting females. Satellites, with their conspicuous pale plumage ornaments, co-display submissively with selected independents and mate opportunistically when their independent partners are momentarily distracted (*21*, *22*). Faeders, the rarest and smallest males, have no ornamental feathers but mimic females in appearance and behavior to sneak copulations (*23*). Breeding males exhibit clear morph variation in circulating androgens (*20*, *24*, *25*). Independents have high circulating testosterone levels but low levels of androstenedione, a less potent androgen and testosterone precursor and metabolite. The nonaggressive satellite and faeder males show the reverse pattern (Fig. 1B). The morphs are differentiated by an autosomal supergene that arose through a chromosomal inversion about 3.8 million years ago (Mya) and harbors about 100 genes, including several involved in steroid metabolism (*20*, *26*). Faeders carry the oldest inversion haplotype whereas the satellite haplotype arose through a rare recombination only 0.07 Mya (*27*). Since one inversion breakpoint is homozygous-lethal, faeders and satellites always carry an ancestral independent haplotype and a derived morph–specific haplotype (*20*, *26*). Here, we capitalize on the existing natural endocrine and genetic contrasts between reproductive morphs to identify and characterize the major genes related to the pronounced androgen differences between males.

Supergene-linked loci show differential expression and allelic imbalance

We sampled adult males from all three morphs during the breeding season, when the differences in androgen levels and social behaviors are most distinct (*20*, *25*). To examine transcriptomic differences, we performed RNA-Seq on tissues highly relevant to behavior or the production/metabolism of sex steroid hormones: brain (seven areas), pituitary glands, adrenal glands, liver and testes. Sampled brain areas comprised nine brain nuclei that include parts of the social behavior network, mesolimbic reward pathway (*28*, *29*), and serotonergic system. These nuclei are either expected to have high expression of sex steroid receptors (preoptic area, lateral septum, nucleus taeniae, hypothalamus), contain major populations of dopamine neurons (ventral tegmental area and substantia nigra), serotonin neurons (raphe), or are involved in executive functions in birds (caudal nidopallium, a putative partial homolog to the mammalian prefrontal cortex) (*30*) (fig. S1). Hypothalamus samples included anterior, ventromedial, lateral, and posterior hypothalamic nuclei (see supplementary materials for details).

Genome-wide, we found a large number of differentially expressed genes in pairwise comparisons of morphs considering all tissues (faeders versus independents: 1762; satellites versus independents: 1438; faeders versus satellites: 1395.) The supergene region had a notable enrichment of differentially expressed genes [faeders versus independents (odds ratio = 8.15, *P*-adjusted = 2.15e-15); satellites versus independents (odds ratio = 5.56, *P*-adjusted = 8.66e-12); faeders versus satellites (odds ratio = 3.05, *P*-adjusted = 6.13e-05)] (Fig. 1, C to E, and table S1). Consistent with the evolutionary histories of their different haplotypes, faeders and independents—which carry the most divergent haplotypes

[1]Max Planck Institute for Biological Intelligence, Seewiesen, Germany. [2]Department of Cognitive and Behavioral Biology, University of Vienna, Vienna, Austria. [3]Institut für Biologie, Freie Universität Berlin, Berlin, Germany. [4]Bioinformatics Solution Center, Freie Universität Berlin, Berlin, Germany. [5]Metabolic Physiology, Institute for Diabetes and Cancer, Helmholtz Munich, German Research Center for Environmental Health, Neuherberg, Germany. [6]Lindenstrasse 9, Allschwil, Switzerland. [7]Research Centre in Biodiversity and Genetic Resources, University of Porto, Vairão, Portugal. [8]Konrad Lorenz Institute of Ethology, University of Veterinary Medicine, Vienna, Austria. [9]Department Biologie II, Ludwig Maximilians University Munich, Martinsried-Planegg, Germany. [10]Department of Biological Sciences, Simon Fraser University, Burnaby, Canada.
***Corresponding author. Email: jasmine.loveland@univie.ac.at (J.L.L.); alex.zemella@bi.mpg.de (A.Z.); clemens.kuepper@bi.mpg.de (C.K.)**
†These authors contributed equally to this work.

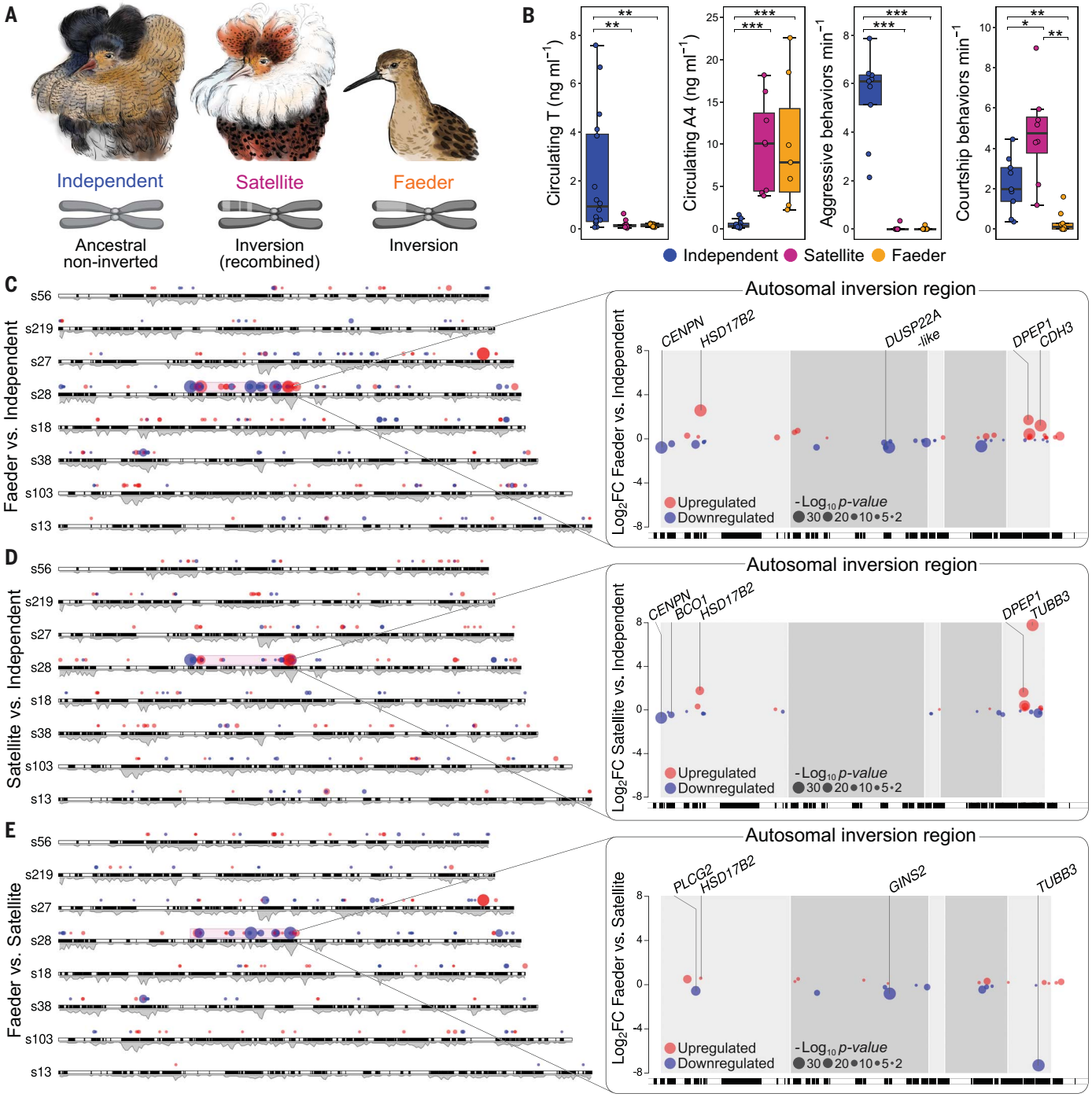

Fig. 1. Gene expression between male morphs is concentrated in the supergene region. (**A**) Male ruff morphs differ in ornamental plumage and supergene haplotypes. (**B**) Morph-specific concentrations of circulating testosterone (n = 36), androstenedione (n = 25), aggression and courtship (n = 26). The morph model differentially expressed genes in pairwise comparisons. (**C**) Faeder versus independent (n = 26). (**D**) Satellite versus independent (n = 27) and (**E**) Faeder versus satellite (n = 19), aligned to karyoplots for a subset of representative scaffolds. The supergene region is magnified on right panels with recently recombined areas shaded in dark gray. Each circle is a differentially expressed gene; red and blue circles denote higher and lower expression levels in the first versus second morph, respectively. The top differentially expressed genes with the largest absolute $\log_2$ fold change are labeled. Karyoplot shading denotes gene presence (black) and absence (white). Gene density plot calculated in 10^5 base pair (bp) windows. Kruskal-Wallis tests followed by Wilcoxon rank tests with Bonferroni adjusted P-values were used in (B), asterisks indicate $^*P < 0.05$, $^{**}P < 0.01$, $^{***}P < 0.001$. (B) modified from (*38*).

(*20*, *26*, *27*)—had the highest number of differentially expressed genes with a relatively even distribution across the inversion region (Fig. 1C). By contrast, there was a notable absence of differentially expressed genes in recently recombined regions of the satellite haplotype in the satellite versus independent comparison (Fig. 1D), although these regions harbored many differentially expressed genes in the faeder versus satellite comparison (Fig. 1E). The spatial pattern of differentially expressed genes suggests an important role for cis regulatory elements

in controlling expression of nearby loci in the inversion region.

Next, we examined variation in gene expression by tissue. Principal component analysis revealed clear clustering and separation by organ and then brain area, with one cluster representing samples from lateral septum and preoptic area, which are adjacent brain areas (fig. S2). Hypothalamus, pituitary, and adrenal glands, three tissues prominently involved in the regulation of systemic androgen levels, stood out with large numbers of differentially expressed genes (fig. S3). In most tissues, comparisons involving independents had more differentially expressed genes than those of the faeder versus satellite comparison (fig. S3).

Recombination between non-inverted and inverted haplotypes is exceptionally rare (*31*), and as a result the derived faeder and satellite haplotypes have accumulated mutations leading to the presence of distinct inversion alleles. This allowed us to quantify allele-specific expression from RNA-Seq data across different tissues (fig. S4). Faeders showed allelic imbalance in 87 of 97 measurable protein-coding genes, spread throughout the entire inversion region. In satellites, we detected imbalance in 68 of 79 measurable protein-coding genes; however, regions that recently recombined with the independent haplotype showed fewer genes with allelic imbalance than the non-recombined regions.

HSD17B2 expression and isozyme variation differentiates ancestral from derived morphs

To identify candidate genes for the distinct variation in circulating androgens between morphs (Fig. 1B), we investigated individual differentially expressed genes associated with the supergene that showed pronounced expression differences between independents and the other two morphs, particularly in tissues related to androgen regulation and metabolism. Differences in circulating androgen concentrations among male morphs may arise from changes in the expression of genes encoding steroidogenic enzymes (*18*, *32*), gonadotropins and their receptors (*33*), or receptors for sex steroids (*34*). However, neither gonadotropin, androgen nor estrogen receptors were differentially expressed among ruff morphs [fig. S5, see also (*24*)]. Instead, the top candidate for morph differentiation was the 17-beta hydroxysteroid dehydrogenase 2 gene (*HSD17B2*), whose enzymatic product converts testosterone to androstenedione, estradiol to estrone, and 20-alpha dihydroprogesterone to progesterone (*35*). HSD17B2 belongs to a large family of more than a dozen highly multifunctional HSD17B enzymes that catalyze conversions between 17-keto steroids and 17-beta hydroxy steroids (*36*, *37*). Although the full HSD17B family has not been extensively studied in birds, ruff HSD17B2 is likely functionally homologous to the human enzyme as all conserved functional domains are present (*38*) and the gene synteny is high.

The ruff *HSD17B2* gene is located within a nonrecombined area of the supergene and stood out among inversion genes because it was a top differentially expressed gene with strong allele-specific expression of the inversion allele in faeders and satellites (Fig. 2A). In multiple tissues—including the hypothalamus, a brain area essential to androgen regulation in vertebrates—*HSD17B2* had lower expression in independents than in satellites or faeders (Fig. 2, B and C). It also showed a strong bias toward the inversion allele in most tissues (Fig. 2D and fig. S4), including all brain areas investigated (range of inversion allele-specific expression proportion in satellites: 80 to 100%; faeders: 91 to 100%) (fig. S4).

The expression bias toward the inversion allele is puzzling because simulation models predicted that inversion haplotypes accumulate deleterious mutations (*39*). The coding sequences for *HSD17B2* show several nonsynonymous mutations, including four amino acid substitutions shared between faeders and satellites (Fig. 3A). Notably, a selection test using a branch model and annotated HSD17B2 sequences from six related Charadriiform species revealed strong selection signatures on the satellite and faeder haplotypes with three of their four shared residues (A235S, L279F, I329T) being positively selected (fig. S6). In addition, the variation in circulating androgens between independents and the two inversion-carrying morphs suggests that the enzymatic activity of HSD17B2 has not deteriorated; on the contrary, it appears to have increased (Fig. 1B).

To evaluate whether and how these mutational changes altered enzymatic function, we investigated the molecular interactions in ruff HSD17B2 variants with testosterone and its cofactor nicotinamide adenine dinucleotide (NAD^+) in silico, and determined their enzymatic kinetics for testosterone conversion through in vitro assays. Since HSD17B2 is anchored in the membrane of the endoplasmic reticulum (*40*), we used a truncated protein structure without amino acids in the transmembrane topology as in (*41*) for the in silico computer simulation. We restricted the comparison to ruff homodimers as they should be the predominant dimers found in faeder and satellite cells, given the widespread allele-specific expression favoring derived *HSD17B2* alleles. The homology models revealed lower $\Delta G_{binding}$ values in satellite and faeder than independent HSD17B2 isozymes, suggesting higher binding affinities for both testosterone and NAD^+ in the two derived isozymes compared to the ancestral isozyme (Fig. 3B). Moreover, in satellite and faeder isozymes, testosterone was closer to the residues that initiate and perform the catalytic reaction, suggesting enhanced substrate binding, catalysis, and product release in derived variants (Fig. 3, C and D).

We then performed enzymatic assays in vitro, comparing ruff homodimers (Fig. 3A). All isozymes retained function but varied in their enzymatic characteristics (Fig. 3, E and F). Satellite and faeder homodimers showed higher maximum velocity (v_{max}) for testosterone conversion than the independent homodimer. The isozymes also showed significant variation in their Michaelis constants (K_M), indicating that the faeder and satellite homodimers require a lower and higher substrate concentration, respectively, than that of the independent to achieve half v_{max}. The resulting utilization rates (v_{max}/K_M) were more than three times higher for the faeder than for the independent homodimer, with the satellite homodimer showing intermediate rates (Fig. 3F). To understand how individual mutations in the faeder and satellite isozymes affect kinetics of the derived variants, we next examined engineered variants (Var-1 to Var-4) with different combinations of the four shared residues for in vitro tests. As previously predicted (*38*), a single amino acid change (L279F, represented by Var-1) led already to a two times greater utilization rate in comparison to the independent isozyme (Fig. 3F).

Androgen and gene expression variation in male testes and blood

The male testes are the primary organs for testosterone synthesis but *HSD17B2* was not differentially expressed in this tissue (Fig. 2C). To examine androgen production in testes, we quantified testosterone and androstenedione concentrations through a radioimmunoassay. Based on the known circulating androgen levels and differences in HSD17B2 activity, we predicted that satellites and faeders would have high levels of androstenedione and low levels of testosterone in testes, and the reverse pattern in independents. Contrary to our expectations, we found that testes of satellites and faeders had, on average, seven to eight times higher testosterone and 20 times higher androstenedione concentrations than independents (Fig. 4A).

To illuminate regulatory variation that may underlie the unexpected testicular androgen profiles of satellites and faeders, we conducted a detailed analysis on gene expression variation between morphs in this tissue. This revealed, first, an overrepresentation of differentially expressed genes with the gene ontology terms "steroid hormone biosynthetic process" and "hormone metabolic processes" in both faeders and satellites, compared with independents (fig. S7). Examining expression differences between the major genes involved in androgen synthesis, we detected high variation during the early catalytic steps in this pathway with higher

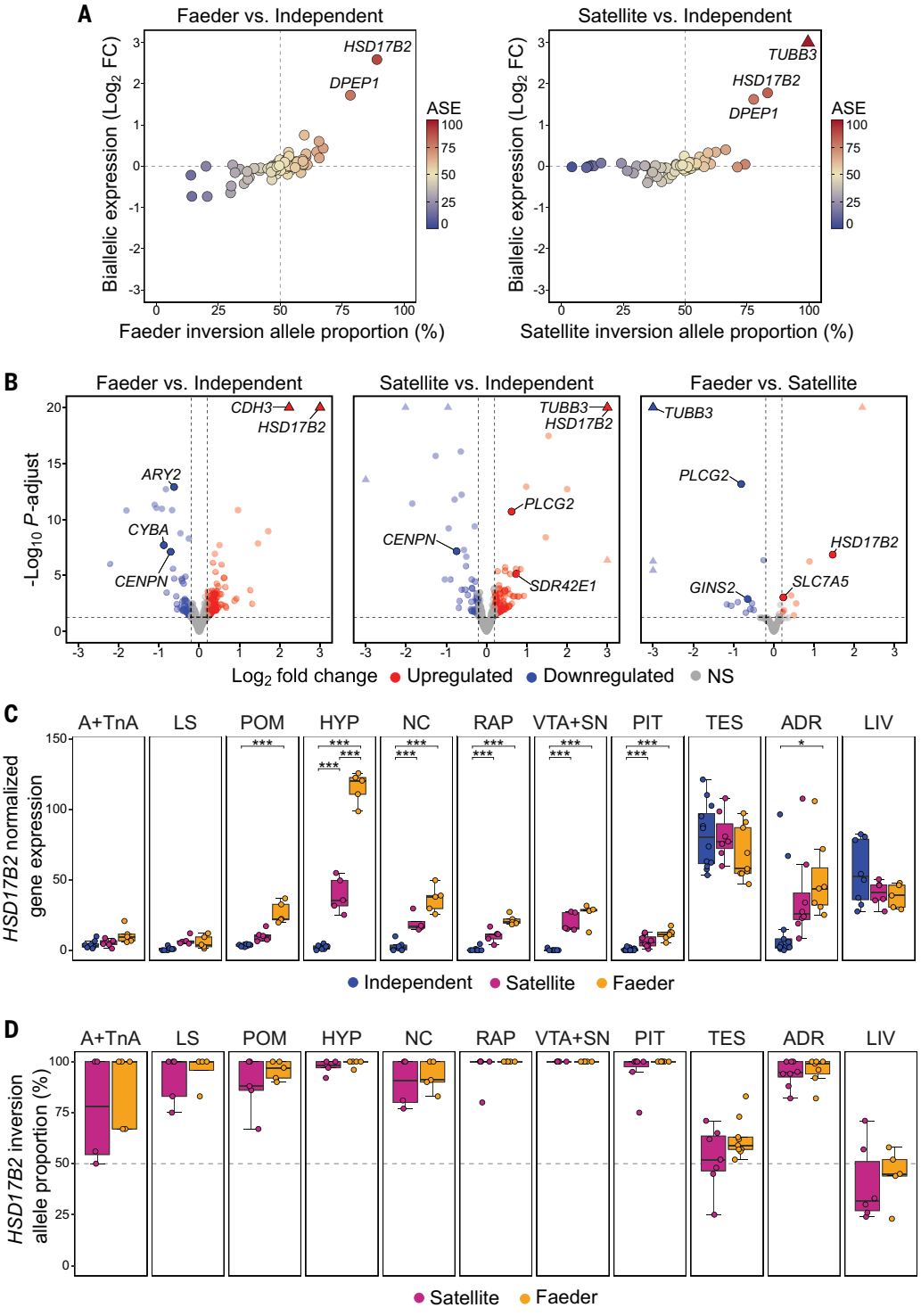

Fig. 2. Differential expression and allelic imbalance in *HSD17B2* across tissues and morphs. (**A**) Gene expression in faeders (*n* [birds, samples] = 9, 63) and satellites (*n* = 10, 63) for loci in inverted regions shown as biallelic expression (log_2 fold change, *y*-axis) relative to independents (*n* = 17, 103) and proportion expressed from respective inversion alleles (*x*-axis). Genes (circles) colored according to inversion allele-specific expression (ASE) bias. Dashed lines represent no difference in gene expression (horizontal) and no allelic bias (vertical). (**B**) Hypothalamic differentially expressed genes (-log_{10} *P*-adjust value >1.25) comparing first and second-listed morph (*n* per plot = 13, 13, 10 birds). Genes with log_2 fold change <−0.2 are shown in blue and log_2 fold change >0.2 are shown in red. NS, nonsignificant. Genes with values beyond axes' ranges are shown as triangles. Labels highlight five inversion genes with the largest absolute log_2 fold change. Tissue-specific *HSD17B2* expression as (**C**) biallelic and (**D**) inversion-allele proportion; *n* [birds, samples] = 36, 229. Asterisks denote differential expression, *P*-values are Benjamini-Hochberg corrected (*P < 0.05, ***P < 0.001). A+TnA, arcopallium and nucleus taeniae; LS, lateral septum; POM, preoptic area; HYP, hypothalamus; NC, caudal nidopallium; RAP, raphe; VTA+SN, ventral tegmental area and substantia nigra; PIT, pituitary; TES, testes; ADR, adrenals; LIV, liver. Brain area details in fig. S1.

expression of *STAR*, *CYP11A1*, and *CYP17A1* in satellites and faeders than in independents (Fig. 4, B and C). Other genes such as *HSD3B2* and even *HSD17B3*—responsible for the reverse conversion of androstenedione to testosterone (Fig. 4B)—were highly but similarly expressed in all three morphs, and we found no evidence of altered expression of genes involved in steroid transport (table S2). This suggests that differentially expressed genes early in the androgen synthesis pathways instigate morph variation in androgens in the testes. Notably, *HSD17B2* was not differentially expressed in testes and its overall expression was about 25 times lower than expression of *HSD17B3* (Figs. 2C and 4C). Our results were fully consistent with an earlier study on morph differences in a few selected genes of the androgen synthesis pathway (*24*) and point to functional requirements such as the need of testosterone for sperm production constraining *HSD17B2* expression variation in testes.

To inspect morph variation in androgens, we compared androstenedione and testosterone concentrations in blood plasma and testes (fig. S8). In independents, we found strong positive relationships between concentrations

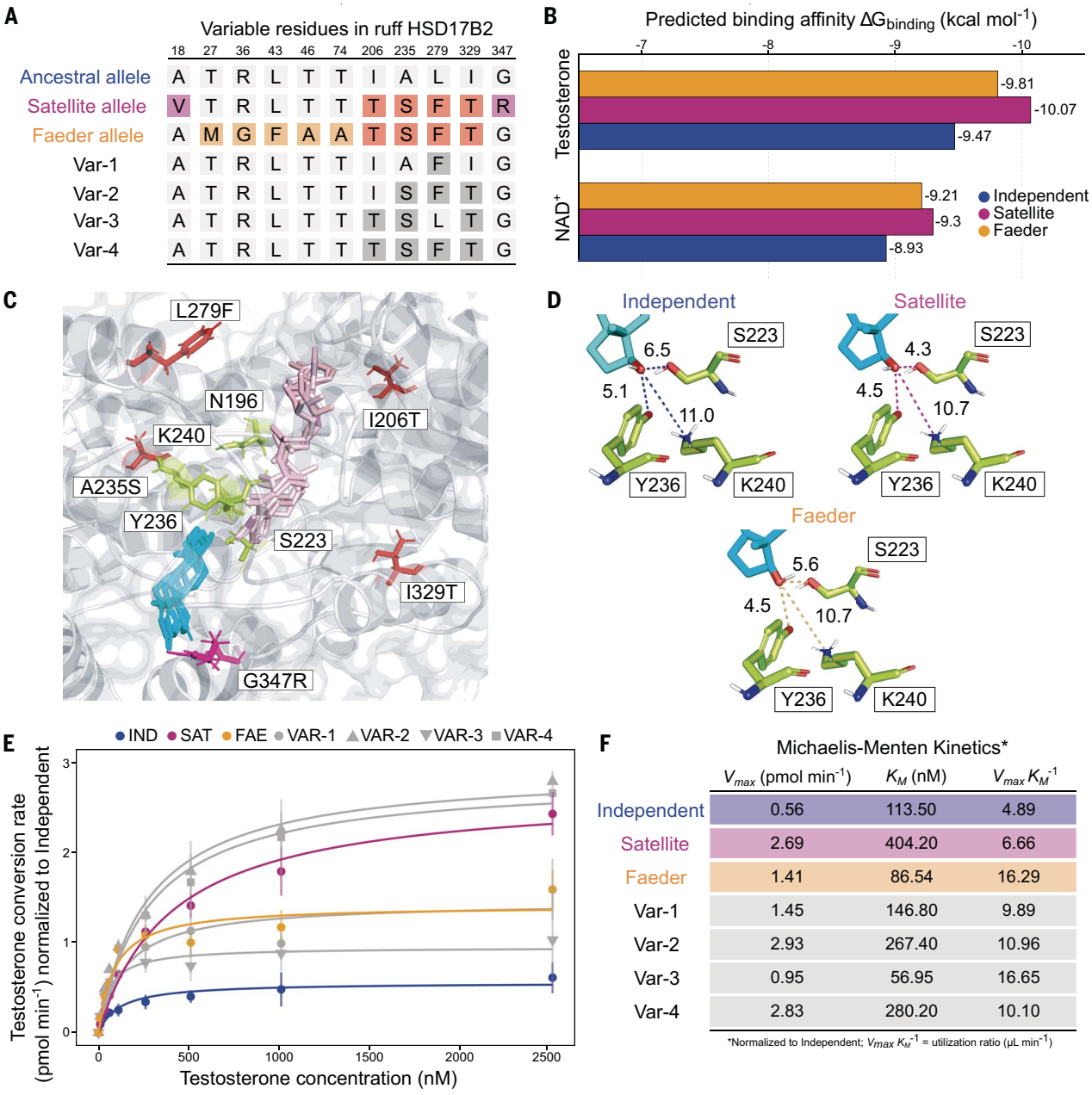

Fig. 3. Derived HSD17B2 isozymes show faster testosterone conversion than the ancestral isozyme. (**A**) Variable residues among ruff HSD17B2 isozymes and engineered mutant variants (Var-1 to Var-4) tested for enzymatic activity. Relative to the ancestral (independent) allele, mutated residues shared by satellite and faeder alleles are in orange; position numbers from XP_014797711.1. (**B**) In silico model predicts better binding affinity (lower values) for testosterone and NAD^+ in faeders and satellites than independents. (**C**) Predicted three-dimensional monomeric structure of independent HSD17B2 (gray) zoomed in to the binding pocket with testosterone (cyan) and NAD^+ (pink). Residues (N196, S223, Y236, K240) from the canonical "NSYK" catalytic tetrad of short chain dehydrogenase/reductase enzymes (light green). Residues that are mutated in satellite and faeder isozymes (red) feature in close vicinity to the binding pocket. (**D**) In silico models reveal shorter atomic distances (in Ångstroms) between testosterone and functional catalytic "SYK" (S223, Y236, K240) sites in satellite and faeder variants, indicating potential for faster catalytic turnover than with the independent variant. (**E**) In vitro rates of testosterone conversion for different isozymes across a range of substrate concentrations. IND, independent; SAT, satellite; FAE, faeder; VAR, variant. Error bars are ±SD from three replicates. (**F**) Michaelis-Menten kinetics calculated from (E).

of both androgens (table S3). In satellites and faeders, this was also the case between androstenedione and testosterone concentrations measured in the testes, but not for correlations involving plasma testosterone, which circulates in very low concentrations in these morphs. One explanation is that *HSD17B2* is differentially expressed in the blood of morphs. However, *HSD17B2* expression and activity in blood is typically either absent or rarely detected (*42*, *43*). To explore this conundrum, we conducted further RNA-Seq in nine males to compare *HSD17B2* expression in blood between morphs. This revealed extreme morph variation in blood *HSD17B2* expression, much higher than in all other tissues examined. Consistent with low activity reported in human blood (*42*, *43*) and their own high circulating testosterone concentrations, *HSD17B2* expression was nearly absent in independents. Conversely, *HSD17B2* was highly expressed in faeders and satellites,

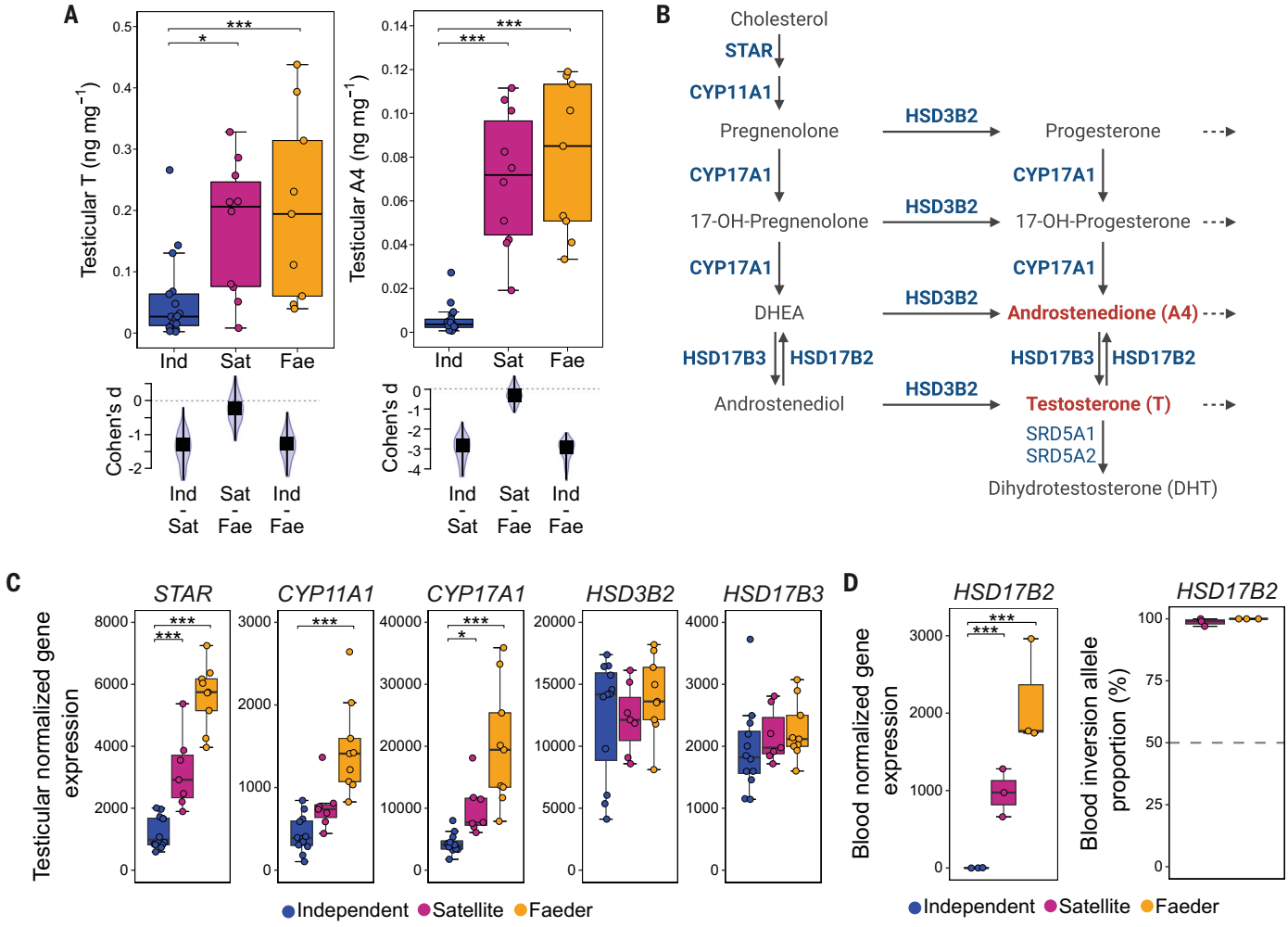

Fig. 4. Sources of androgen variation between male morphs in testes and blood. (**A**) Morph-specific testicular testosterone and androstenedione levels including effect sizes (Cohen's d) for pairwise comparisons (n = 36). (**B**) Simplified androgen biosynthesis pathway showing key enzymes responsible for steps from cholesterol to testosterone. (**C**) Testicular expression of genes shown in bold in (B) (n = 28). (**D**) Blood *HSD17B2* expression and allele-specific expression (n = 9). Asterisks denote statistically clear differences, P-values are Benjamini-Hochberg corrected (*P < 0.05, **P < 0.01, ***P < 0.001). Ind, independent; Sat, satellite; Fae, faeder.

with a strong bias toward the derived allele (Fig. 4D). It remains unclear which blood cells overexpress *HSD17B2* in faeder and satellites because, unlike mammals, red blood cells in birds are nucleated. This localized hyperactivity of HSD17B2 in the blood of the two low testosterone morphs may represent an evolutionary innovation that effectively limits the pleiotropic actions of testosterone outside of the testes. High HSD17B2 activity in the blood and hypothalamus of faeders and satellites then results in fast metabolism of testosterone and alters the HPG feedback loop that controls testicular androgen synthesis.

Taken together, our findings imply that a combination of changes in regulation and coding sequence of the *HSD17B2* gene resulted in increased testosterone conversion of derived variants. The supergene-induced suppression of recombination likely accelerated the evolution of the derived variants. The changes of this single gene are expected to have widespread consequences through genetic and hormonal pleiotropy. First, HSD17B2 itself is multifunctional and metabolizes other sex steroids in addition to testosterone (*44*). One of these, estradiol, is also required to mediate effects on territorial mating behaviors in many bird species (*45*–*47*). Future studies should examine how the changes to HSD17B2 affect the conversion rates of its other substrates. Second, the substrates of HSD17B2 are highly pleiotropic signaling molecules that coordinate physiological and developmental processes and can foster the evolution of correlated traits (*48*–*51*). Vertebrate genomes contain hundreds to thousands of response elements for sex steroid receptors that may alter gene expression (*52*, *53*). For example, the swift metabolization of testosterone in the blood of low testosterone morphs will starve androgen receptors in target tissues of one of their most significant ligands and severely affect systemic responses that have evolved over millions of years. In the case of ruffs, the changes in circulating androgens may underlie the profound differences in male aggression that exist between morphs and may be at the heart of the pronounced sexual antagonism that has been introduced by the inversion alleles (*54*). Identifying how androgen levels are altered genetically opens new avenues for understanding the evolution of diverse reproductive phenotypes, antagonistic pleiotropy, and the regulation of social behaviors.

REFERENCES AND NOTES

1. R. F. Oliveira, *Adv. Stud. Behav.* **34**, 165–239 (2004).
2. M. Hau, *BioEssays* **29**, 133–144 (2007).
3. L. Fusani, *Horm. Behav.* **54**, 227–233 (2008).
4. W. Goymann, J. C. Wingfield, *Behav. Ecol.* **25**, 685–699 (2014).

5. D. J. Handelsman, A. L. Hirschberg, S. Bermon, *Endocr. Rev.* **39**, 803–829 (2018).
6. N. L. Staub, M. De Beer, *Gen. Comp. Endocrinol.* **108**, 1–24 (1997).
7. E. D. Ketterson, V. Nolan Jr., M. Sandell, *Am. Nat.* **166**, S85–S98 (2005).
8. N. Sinnott-Armstrong, S. Naqvi, M. Rivas, J. K. Pritchard, *eLife* **10**, e58615 (2021).
9. W. Goymann, *Gen. Comp. Endocrinol.* **163**, 149–157 (2009).
10. M. Mokkonen, E. Koskela, T. Mappes, S. C. Mills, *J. Anim. Ecol.* **81**, 277–283 (2012).
11. R. F. Oliveira, M. Taborsky, H. J. Brockmann, Eds., *Alternative Reproductive Tactics: An Integrative Approach* (Cambridge Univ. Press, 2008).
12. J. E. Mank, *Nat. Rev. Genet.* **24**, 44–52 (2023).
13. A. T. Pavitt, C. A. Walling, J. M. Pemberton, L. E. B. Kruuk, *Biol. Lett.* **10**, 20140685 (2014).
14. V. Bogaert *et al*., *Clin. Endocrinol. (Oxf.)* **69**, 129–135 (2008).
15. C. Ohlsson *et al*., *PLOS Genet.* **7**, e1002313 (2011).
16. K. S. Ruth *et al*., *Nat. Med.* **26**, 252–258 (2020).
17. E. D. Ketterson, J. W. Atwell, J. W. McGlothlin, *Integr. Comp. Biol.* **49**, 365–379 (2009).
18. K. A. Rosvall, C. M. Bergeon Burns, S. P. Jayaratna, E. K. Dossey, E. D. Ketterson, *Integr. Comp. Biol.* **56**, 225–234 (2016).
19. K. K. Soma, N. M. Rendon, R. Boonstra, H. E. Albers, G. E. Demas, *J. Steroid Biochem. Mol. Biol.* **145**, 261–272 (2015).
20. C. Küpper *et al*., *Nat. Genet.* **48**, 79–83 (2016).
21. A. J. Hogan-Warburg, *Ardea* **54**, 109–229 (1966).
22. J. D. M. Tolliver, K. Kupán, D. B. Lank, S. Schindler, C. Küpper, *Anim. Behav.* **197**, 131–154 (2023).
23. J. Jukema, T. Piersma, *Biol. Lett.* **2**, 161–164 (2006).
24. J. L. Loveland, D. B. Lank, C. Küpper, *Front. Genet.* **12**, 641620 (2021).
25. J. L. Loveland *et al*., *Horm. Behav.* **127**, 104877 (2021).
26. S. Lamichhaney *et al*., *Nat. Genet.* **48**, 84–88 (2016).
27. J. Hill *et al*., *Mol. Biol. Evol.* **40**, msad224 (2023).
28. J. L. Goodson, *Horm. Behav.* **48**, 11–22 (2005).
29. L. A. O'Connell, H. A. Hofmann, *Science* **336**, 1154–1157 (2012).
30. K. von Eugen, S. Tabrik, O. Güntürkün, F. Ströckens, *J. Comp. Neurol.* **528**, 2929–2955 (2020).
31. M. Kapun, T. Flatt, *Mol. Ecol.* **28**, 1263–1282 (2019).
32. K. A. Rosvall, C. M. Bergeon Burns, S. P. Jayaratna, E. D. Ketterson, *Horm. Behav.* **84**, 1–8 (2016).
33. I. T. Huhtaniemi, I. T. Huhtaniemi; Themmen APN, *Endocr. Rev.* **21**, 551–583 (2000).
34. J. R. Merritt *et al*., *Proc. Natl. Acad. Sci. U.S.A.* **117**, 21673–21680 (2020).
35. L. Wu *et al*., *J. Biol. Chem.* **268**, 12964–12969 (1993).
36. R. Mindnich, G. Möller, J. Adamski, *Mol. Cell. Endocrinol.* **218**, 7–20 (2004).
37. C. Prehn, G. Möller, J. Adamski, *J. Steroid Biochem. Mol. Biol.* **114**, 72–77 (2009).
38. J. L. Loveland, L. M. Giraldo-Deck, A. M. Kelly, *Front. Physiol.* **13**, 1011629 (2022).
39. E. L. Berdan, A. Blanckaert, R. K. Butlin, C. Bank, *PLOS Genet.* **17**, e1009411 (2021).
40. M. Tsachaki, J. Birk, A. Egert, A. Odermatt, *Biochim. Biophys. Acta* **1853**, 1672–1682 (2015).
41. C. P. Sager *et al*., *J. Steroid Biochem. Mol. Biol.* **206**, 105790 (2021).
42. L. Schiffer *et al*., *Eur. J. Endocrinol.* **184**, 353–363 (2021).
43. Z. Zhou, C. H. L. Shackleton, S. Pahwa, P. C. White, P. W. Speiser, *Mol. Cell. Endocrinol.* **138**, 61–69 (1998).
44. S. Andersson, N. Moghrabi, *Steroids* **62**, 143–147 (1997).
45. G. F. Ball, J. Balthazart, *Physiol. Behav.* **83**, 329–346 (2004).
46. L. Fusani, M. Gahr, J. B. Hutchison, *Gen. Comp. Endocrinol.* **122**, 23–30 (2001).
47. J. T. Watson, E. Adkins-Regan, *Horm. Behav.* **23**, 432–447 (1989).
48. T. Flatt, M.-P. Tu, M. Tatar, *BioEssays* **27**, 999–1010 (2005).
49. J. W. McGlothlin, E. D. Ketterson, in *Snowbird: Integrative Biology and Evolutionary Diversity in the Junco*, E. D. Ketterson, J. W. Atwell, Eds. (Univ. of Chicago Press, 2016), pp. 100–119.
50. T. N. Wittman, C. D. Robinson, J. W. McGlothlin, R. M. Cox, *Evol. Lett.* **5**, 397–407 (2021).
51. B. Dantzer, E. M. Swanson, *Integr. Comp. Biol.* **57**, 372–384 (2017).
52. R. M. Cox, *Mol. Cell. Endocrinol.* **502**, 110668 (2020).
53. B. Gegenhuber, M. V. Wu, R. Bronstein, J. Tollkuhn, *Nature* **606**, 153–159 (2022).
54. L. M. Giraldo-Deck *et al*., *Nat. Commun.* **13**, 1384 (2022).
55. A. Zemella, azemella/Ruff_adults_RNASeq_gene_expression_2024: Update MD analysis and results, v6.0.0, Zenodo (2024); https://zenodo.org/records/14056330.

ACKNOWLEDGMENTS

We thank M. Trappschuh for technical assistance in steroid quantifications, S. Roilo for assistance in sample collection, and C.D. Corrales Parada for help with behavioral coding. M. Hau und H. Brumm kindly provided comments on an earlier draft. Y. Pei provided the artwork in Fig. 1A. **Funding:** This work was supported by a sequencing grant from the German Research Foundation (DFG) (KU 3051/2-1) (to C.K., K.N.); a grant by the Austrian Science Fund (FWF) (M3302-B) (to J.L.L.); Helmholtz Munich, German Research Center for Environmental Health; the National Science and Engineering Research Council of Canada (NSERC) (to D.B.L.); and the Max Planck Society. The sequencing was done in the scope of the DFG-funded NGS-Competence Network by the Dresden-concept Genome Center, c/o Center for Molecular and Cellular Bioengineering (CMCB), Technology Platform of the TUD Dresden University of Technology, 01062 Dresden, Germany and MPI-CBG, Pfotenhauerstr. 108, 01307 Dresden, Germany. **Author contributions:** J.L.L., A.Z., V.M.J., G.M., B.B., J.T., and W.G. generated and analyzed the data. J.L.L. and L.M.G.-D. collected tissues. D.B.L. raised and maintained the captive birds. M.G., L.F., and K.A.D. provided reagents and dedicated infrastructure. C.K., K.N., J.L.L., and D.B.L. obtained funds. C.K., K.N., and J.L.L. supervised the work. C.K. conceived the study. C.K., J.L.L., and A.Z. wrote the initial manuscript. All authors edited and approved the final manuscript. **Competing interests:** Authors declare that they have no competing interests. **Data and materials availability:** The RNA sequencing data have been uploaded to NCBI under the BioProject PRJNA1099138. Plasmid accession codes and identifiers of publicly available genomic data are listed in materials and methods and table S8. All code and materials used in the analysis are available at Zenodo (*55*).

SUPPLEMENTARY MATERIALS

science.org/doi/10.1126/science.adp5936
Materials and Methods
Figs. S1 to S11
Tables S1 to S8
References (*56*–*97*)
MDAR Reproducibility Checklist

Submitted 23 April 2024; accepted 26 November 2024
10.1126/science.adp5936